Journal of the European Ceramic Society 21 (2001) 2509–2514
www.elsevier.com/locate/jeurceramsoc

Synthesis and characterization of Fe and P substituted 3:2 mullite

S. Ronchetti[a,*], M. Piana[a], A. Delmastro[a], M. Salis[b], D. Mazza[a]

[a]*Dipartimento di Scienza dei Materiali ed Ingegneria Chimica, Politecnico di Torino, Corso Duca degli Abruzzi 24, 10129 Torino, Italy*
[b]*Istituto di Fisica Superiore, Università di Cagliari, Via Ospedale 72, Cagliari, Italy*

Abstract

The incorporation in mullite structure of foreign elements has been studied since 1924. In this paper the isovalent $\frac{1}{2}$P plus $\frac{1}{2}$Al for Si substitution has been investigated employing wet chemistry preparative route with a final firing temperature of 1300°C. The extent of solid solution and the crystallographic features of the end term with composition $Al_{6.22}Si_{1.56}P_{0.22}O_{13}$ are described on the basis of XRPD profile fitting. This substitution has also been examined in the presence of the contemporary Fe for Al substitution; the end term of this coupled isovalent compositional series $Al_{5.90}Fe_{0.20}Si_{1.80}P_{0.10}O_{13}$ has been characterized too. In this latter case, the crystallographic results are confirmed by Mössbauer spectroscopy. The simple Fe for Al substitution at 1300°C has also been re-examined in the same preparative conditions. The composition and the structure of the end term ($Al_{5.60}Fe_{0.40}Si_2O_{13}$) are in agreement with previous studies. The incorporation degree of Fe and P in the coupled substitution results in being approximately halved in respect to simple substitutions of the two elements.

Keywords: Mullite; Spectroscopy

1. Introduction

The resemblance of mullite structure to the sillimanite one is a reason for its recognition as a distinct phase only, by Bowen and Greig in 1924,[1] despite its natural, even if rare, presence in rocks and its formation in fired clay products for centuries. It has indeed an intermediate composition between sillimanite Al_2SiO_5 and alumina Al_2O_3, namely its stability field varies between $Al_6Si_2O_{13}$ (3:2 mullite) and Al_4SiO_8 (2:1 mullite); this is usually resumed with the formula $Al_{4+2x}Si_{2-2x}O_{10-x}$ ($0.25 \leqslant x \leqslant 0.4$). In order to accommodate this compositional variation, the exchange $2Al^{3+} + \square \rightarrow 2Si^{4+} + O^{2-}$ ($\square$ = oxygen vacancy) takes place, to an extent which depends on temperature as well as the preparative route.

The resolution of a mullite average crystal structure by X-ray diffraction dates back only to the sixties of the last century in the studies by Sadanaga et al.,[2] Burnham [3] and Durovic.[4] Angel and Prewitt [5] carried out an accurate structural study of a member of the mullite solid solution. The mullite phase, with its compositional variation, may be thought as stemming from the sillimanite Al_2SiO_5 by means of the substitution $2Al^{3+} + \square \rightarrow 2Si^{4+} + O^{2-}$; in the resulting structure the cell edge c is halved, while a and b undergo a small change. The chains formed by edge sharing octahedra AlO_6 running parallel to the c axis remain unchanged from sillimanite; however, the double chains of tetrahedra SiO_4 or AlO_4, cross-linking the octahedron columns, are readjusted because of the removal of linking tetrahedra oxygens (Oc site). In fact, to complete its coordination, the cation in a tetrahedral site T adjacent to the vacancy moves itself toward an occupied Oc site, giving up a new tetrahedral site designated T*. The neighbouring occupied Oc site is now co-ordinated to three tetrahedral cations, so the oxygen shifts off the special position into a general one, designated Oc*, towards the T* site. So this structure can be defined as a modified defect structure of sillimanite.

Beyond this fundamental substitution other different ones are possible indeed. Iron and titanium were the first elements investigated, during a research on solid solution between mullite and Fe_2O_3, TiO_2 .[6] W. E. Brownell [7] in 1958 showed the shifts of the mullite X-ray diffraction lines with Fe_2O_3 solid solution and asserted that the trivalent iron assumes the position of the trivalent aluminium on the basis of valence and ionic size resemblance. Murthy and Hummel [8] measured the changes in lattice parameters and unit cell volume of solid solution of TiO_2, Fe_2O_3 and Cr_2O_3 in 3:2 mullite as a function of composition and temperature. Assuming that Fe^{3+} ions have an ionic radius larger than Al^{3+}, they expected the Fe^{3+} to go into the main octahedral chains.

More recently Schneider and Rager [9] published their thorough studies on the mode of iron incorporation in synthetic sinter and commercially fused mullites. In sinter mullites they found three Fe3+ centres, corresponding to iron in octahedral (generally a great deal), tetrahedral site

* Corresponding author.
E-mail address: ronchett@athena.polito.it (S. Ronchetti).

0955-2219/01/$ - see front matter
PII: S0955-2219(01)00272-2

and cluster, the last assigned on the basis of the occurrence of superparamagnetic phases (EPR evidence). Only very low iron content is incorporated in fused mullites, almost exclusively as Fe^{3+} at the tetrahedral lattice site.

Chaudhuri and Patra [10] synthesized pure and transition metal ion doped mullite with a preparative method similar to that presented in this paper, i.e. by co-precipitating hydroxides of Al, Si and of the substituting ions (Mn, Fe, Cr and Ti) with ammonia, using as starting materials water soluble salts and organometallic compounds. Their conclusions on site occupation of the substituting ions are based on indirect evidence on change of cell edges, cell volume and crystal habit with ion incorporation.

Generally speaking, the different substitution elements can be classified according to their ionic size. Transition metals with ionic radius in the range 0.54–0.62 Å (like Ti^{4+}, Ti^{3+}, Fe^{3+}, Cr^{3+}, and others) preferably replace Al at the elongated octahedrons. The substitution occurs, up to a certain extent, which depends on the final firing temperature, with a limit of about 10–11 at.% at 1600°C. Larger elements, like Ni^{2+}, Co^{2+}, Cu^{2+}, do not enter the mullite lattice, but may promote the formation of mullite, without being incorporated into its structure.[11] Smaller elements, like B, can be easily incorporated on tetrahedral sites of the mullite structure, according to isovalent substitutions:[12] $\frac{1}{2}B^{3+}$ (0.12 Å) + $\frac{1}{2}P^{5+}$ (0.17 Å) → Si^{4+} (0.26 Å), in which brackets indicate ionic radii in fourfold coordination according to Shannon and Prewitt.[13] This latter kind of mullite is stable between 900 and 1000°C only in a certain composition: monophasic Al_8BPO_{16} derives formally from Al_4SiO_8 (2:1 mullite) while attempts to prepare substituted 3:2 mullite (Al_6BPO_{13}) yields biphasic admixtures. The systematic study of the ternary system Al_2O_3–B_2O_3–P_2O_5 has allowed the determination of the stability range as $Al_{8+y}B_{1+y}P_{1-y}O_{16+y/2}$ with y varying from 0 to 0.6.

In this paper we investigate the isovalent substitution of ($\frac{1}{2}Al^{3+} + \frac{1}{2}P^{5+}$) for Si^{4+} in 3:2 mullite, in the presence or absence of simultaneous Fe^{3+} for Al^{3+} substitution. In order to compare with previous results, the simple Fe^{3+} for Al^{3+} substitution was also re-examined in the same preparative conditions. The examined stoichiometries may be expressed by:

$\frac{1}{2}Al^{3+} + \frac{1}{2}P^{5+} \rightarrow Si^{4+}$ (Series 1) $Al_{6+y/2}Si_{2-y}P_{y/2}O_{13}$ $(0 < y < 0.6)$

$Fe^{3+} \rightarrow Al^{3+}$ (Series 2) $Al_{6-y}Fe_ySi_2O_{13}$ $(0 < y < 0.80)$

$\frac{1}{2}Al^{3+} + \frac{1}{2}P^{5+} \rightarrow Si^{4+}$ $Fe^{3+} \rightarrow Al^{3+}$ (Series 3) $Al_{6-y/2}Fe_ySi_{2-y}P_{y/2}O_{13}$ $(0 < y < 0.33)$

2. Experimental

2.1. Samples preparation

The substituted mullites were obtained by sol-gel synthesis. Starting materials were $Al(NO_3)_3 \cdot 9H_2O$ (Fluka 99.9% purity), tetraethylorthosilicate (TEOS, Aldrich 99%), $Fe(NO_3)_3$ and $(NH_4)H_2PO_4$ (Fluka, 99.0%).

A measured volume of TEOS is added to an equal volume of ethanol (95%) and half a volume of distilled water. The pH of the aqueous alcoholic phase is adjusted to 0.5–1.0 with a few drops of HNO_3. In this way a clear solution (A) is quickly obtained after some minutes of stirring at room temperature. The "r" factor (i.e. water moles/TEOS moles) reaches a value of about 7. Under these conditions TEOS firstly is partially hydrolysed to silanol monomers.[14]

An aqueous solution (B) is obtained by admixing ammonium diacid phosphate, Al and Fe nitrates in stoichiometric amount, adding 10 wt.% of reducing agent (glycerol) to promote the decomposition of nitrates. The solution B is added to A and the clear solution thus obtained is then treated with excess aqueous ammonia (30 wt.%). Condensation and cross linking of silanol monomers rapidly occurs, whilst aluminium and iron hydroxides precipitate, thus obtaining a complete gelation. The gel so obtained is first dried at 150°C, at which temperature nitrates begin to decompose with a redox reaction, emitting brown coloured gases (NO_x, CO, CO_2 and H_2O). After completion of the reaction, the obtained spongy, bulky solid is then transferred into a 400°C and then 500°C oven for 30 min, in order to completely remove nitrogen oxides and to oxidize the remaining organic residues. The resulting xerogels are amorphous when examined by X-ray diffraction. In these materials the degree of mixing between the component oxides is on the nanometer scale, as indicated by the low crystallization temperatures found in this work and confirmed by previous research.[11] These xerogels were examined by simultaneous DTA/TG (Setaram TG92) in order to assess the crystallization temperature (indicated by a sharp exothermal heat flow) and to check the eventual weight loss at high temperature.

In Fig. 1 is reported the DTA/TG curve of the sample $Al_{6.1}Si_{1.8}P_{0.1}O_{13}$; at 990°C a first exothermic process occurs, relative to the partial crystallization from the

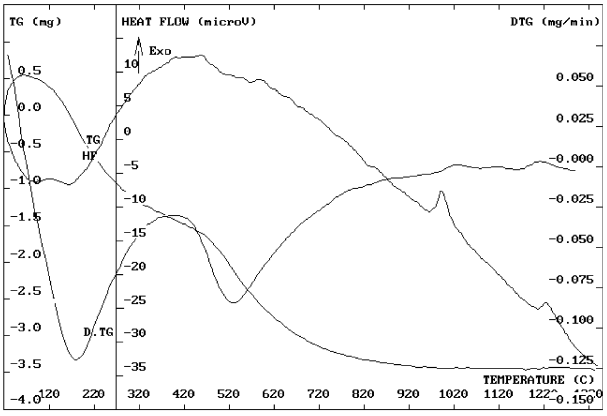

Fig. 1. Simultaneous DTA and TG analysis of sample $Al_{6.1}Si_{1.8}P_{0.1}O_{13}$.

amorphous mass of α-Al_2O_3, whereas the stoichiometric 3:2 mullite only forms at 1225°C, as indicated by a second exothermic process, by reaction of γ-Al_2O_3 with the remaining SiO_2. The weight loss of the amorphous mass is evidenced between 400 and 800°C and after crystallization the weight is constant up to 1300°C.

As shown in Fig.1 no weight loss due to P_2O_5 sublimation is noticeable from 800 to 1300°C. Microprobe analysis (Philips PW 6703, 30 kV, 200 μA) was carried out in order to evidence a possible stoichiometry deviation during preparation. The results confirm the starting composition within a ±3% tolerance. This fact, together with the TG evidence, assures starting composition for the samples up to 1300°C.

On the basis of DTA/TG evidence the solids obtained were carefully ground in agate planetary mixer, pressed into tablets (with a pressure of 3 kbar) and finally heated in air at 1300°C for 2 h in an electric furnace.

2.2. Samples characterization

Tables 1–3 show the phases composition of the samples as synthesized at 1300°C, as resulting from XRPD evidence.

The monophasic samples with limited composition, namely 1D, 2C and 3A, were submitted to X-ray profile fitting. The diffraction patterns were obtained using a Philips X'Pert-MPD powder diffractometer, CuK_α radiation and a curved graphite secondary monochromator. The data were collected in the 2θ-range between 10 and 100°. The XRD patterns gave no evidence of co-existing amorphous phase (broadened background halo) up to the sensitivity of the instrument.

Table 1
Composition of the samples 1A–1F, with the y value in the general formula $Al_{6+y/2}Si_{2-y}P_{y/2}O_{13}$ and the phases present at 1300°C

Sample	Composition	y	Phase(s) at 1300°C
1A	$Al_6Si_2O_{13}$	0	Mullite
1B	$Al_{6.1}Si_{1.8}P_{0.1}O_{13}$	0.2	Mullite-like phase
1C	$Al_{6.2}Si_{1.6}P_{0.2}O_{13}$	0.4	Mullite-like phase
1D	$Al_{6.22}Si_{1.56}P_{0.22}O_{13}$	0.44	Mullite-like phase
1E	$Al_{6.28}Si_{1.44}P_{0.28}O_{13}$	0.56	Mullite-like phase + $AlPO_4$ tridymite
1F	$Al_{6.3}Si_{1.4}P_{0.3}O_{13}$	0.6	Mullite like phase + $AlPO_4$ tridymite

Table 2
Composition of the samples 2A–2E, with the y value in the general formula $Al_{6-y}Fe_ySi_2O_{13}$ and the phases present at 1300°C

Sample	Composition	y	Phase(s) at 1300°C
2A	$Al_6Si_2O_{13}$	0	Mullite
2B	$Al_{5.73}Fe_{0.27}Si_2O_{13}$	0.27	Mullite-like phase
2C	$Al_{5.60}Fe_{0.40}Si_2O_{13}$	0.40	Mullite-like phase (+ Fe_2O_3 traces)
2D	$Al_{5.47}Fe_{0.53}Si_2O_{13}$	0.53	Mullite-like phase + Fe_2O_3
2E	$Al_{5.20}Fe_{0.80}Si_2O_{13}$	0.80	Mullite-like phase + Fe_2O_3

Table 3
Composition of the samples 3A–3C, with the y value in the general formula $Al_{6-y/2}Fe_ySi_{2-y}P_{y/2}O_{13}$ and the phases present at 1300°C

Sample	Composition	y	Phase(s) at 1300°C
3A	$Al_{5.90}Fe_{0.20}Si_{1.80}P_{0.10}O_{13}$	0.20	Mullite-like phase
3B	$Al_{5.87}Fe_{0.27}Si_{1.73}P_{0.13}O_{13}$	0.27	Mullite-like phase + $AlPO_4$ tridymite
3C	$Al_{5.83}Fe_{0.33}Si_{1.67}P_{0.16}O_{13}$	0.33	Mullite-like phase + $AlPO_4$ tridymite

Two samples iron-substituted (2D and 3B) were subjected to Mössbauer spectroscopy analysis at room temperature by means of a ^{57}Co γ-ray source. The peaks in the obtained spectra were deconvoluted considering the superposition of two doublets, attributed to iron in octahedral and tetrahedral environment. The results are illustrated in Fig. 2 and in Table 4.

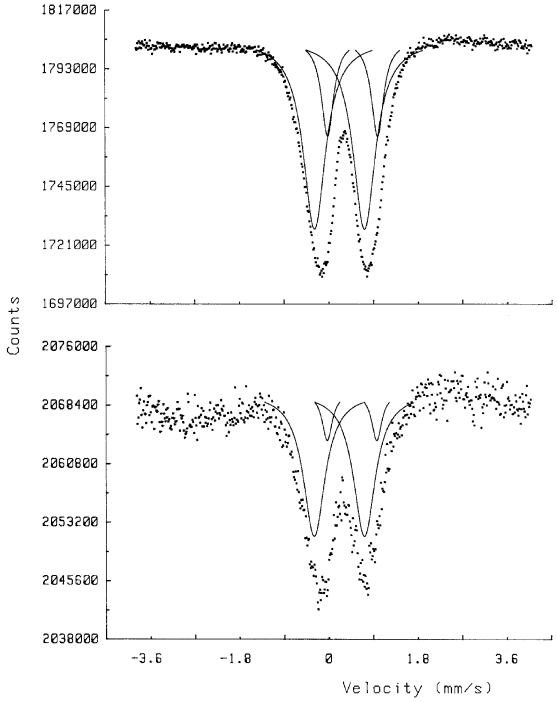

Fig. 2. Mössbauer spectra and their deconvolution relative to sample 2D (above) and 3B (below).

Table 4
Isomer shifts and quadrupole splitting resulting from deconvolution of Mössbauer spectra relative to 2D and 3B, using two doublet

Sample	Tetrahedral doublet		Octahedral doublet	
	Isomer shift (mm/s)	Quadrupole splitting (mm/s)	Isomer shift (mm/s)	Quadrupole splitting (mm/s)
2D	0.221(1)	1.010(1)	0.4863(1)	1.010(1)
3B	0.221(1)	1.022(1)	0.466(1)	1.003(1)

The diffraction data were processed for Rietveld analysis with GSAS,[15] a software package for the refinement of crystal structures.

The refinement strategy in space group Pbam (*n*. 55) started from fitting of background, cell parameters and peak profiles, in this order, using as structural model that one resulting from the study of 2:1 mullite by Angel and Prewitt; as soon as a satisfactory profile fitting was reached, the atomic coordinates were released. The site occupancies were then refined, under the constraint of known preparative stoichiometry. Eventually displacement factors and theta zero correction were refined. The values of atomic displacement factors of different elements in the same site were constrained to be equal.

The results of Rietveld analysis for the three limit compositions are summarised in Tables 5–9. the profile relative to the refinement of sample 1D is shown (Fig. 3). The values of the residual functions for the refinements are: for sample 1D $R_F = 3.92\%$ $R_p = 4.75\%$, for sample 2C $R_F = 3.94\%$ $R_p = 5.22\%$ and for sample 3A $R_F = 5.19\%$ $R_p = 5.54\%$.

Table 5
Results of lattice parameters refinement for the samples analysed and comparison with reference[5] 2:1 mullite

Sample	*a* (Å)	*b* (Å)	*c* (Å)
1D	7.5722(4)	7.6960(4)	2.8856(1)
2C	7.5693(2)	7.7159(2)	2.89470(5)
3A	7.5673(2)	7.7016(2)	2.88895(6)
Ref. 5	7.5785(6)	7.6817(7)	2.8864(3)

Table 6
Structural results of the refinement on sample 1D ($Al_{6.22}Si_{1.56}P_{0.22}O_{13}$)

	Wyckoff site	*x*/*a*	*y*/*b*	*z*/*c*	Fractional occupancy	U_{iso} (Å^3)
Al (1)	2a	0	0	0	1.000	0.0094(7)
Al-T	4h	0.1497(2)	0.3401(3)	$\frac{1}{2}$	0.537(2)	0.0077(6)
Si-T	4h	0.1497(2)	0.3401(3)	$\frac{1}{2}$	0.250(2)	0.0077(6)
P-T	4h	0.1497(2)	0.3401(3)	$\frac{1}{2}$	0.041(2)	0.0077(6)
Al-T*	4h	0.267(1)	0.208(1)	$\frac{1}{2}$	0.130(2)	0.009(3)
Si-T*	4h	0.267 (1)	0.208(1)	$\frac{1}{2}$	0.043(2)	0.009(3)
P-T*	4h	0.267 (1)	0.208(1)	$\frac{1}{2}$	0.000(2)	0.009(3)
Od	4g	0.1286(4)	0.2193(3)	0	1.000	0.012(1)
Oab	4h	0.3560(4)	0.4218(3)	$\frac{1}{2}$	1.000	0.0097(9)
Oc	2d	$\frac{1}{2}$	0	$\frac{1}{2}$	0.62(2)	0.023(2)
Oc*	4h	0.432(4)	0.070(5)	$\frac{1}{2}$	0.13(1)	0.024(8)

Table 7
Structural results of the refinement on sample 2C ($Al_{5.6}Fe_{0.4}Si_2O_{13}$)

	Wyckoff site	*x*/*a*	*y*/*b*	*z*/*c*	Fractional occupancy	U_{iso} (Å^3)
Al (1)	2a	0	0	0	0.929(3)	0.0076(5)
Fe (1)	2a	0	0	0	0.071(3)	0.0076(5)
Al-T	4h	0.1483(2)	0.3408(2)	$\frac{1}{2}$	0.491(2)	0.0085(5)
Fe-T	4h	0.1483(2)	0.3408(2)	$\frac{1}{2}$	0.038(1)	0.0085(5)
Si-T	4h	0.1483(2)	0.3408(2)	$\frac{1}{2}$	0.303(2)	0.0085(5)
Al-T*	4h	0.266(1)	0.205(1)	$\frac{1}{2}$	0.094(2)	0.015(3)
Fe-T*	4h	0.266(1)	0.205(1)	$\frac{1}{2}$	0.002(1)	0.015(3)
Si-T*	4h	0.266(1)	0.205(1)	$\frac{1}{2}$	0.072(2)	0.015(3)
Od	4g	0.1258(3)	0.2203(3)	0	1.000	0.0110(9)
Oab	4h	0.3579(3)	0.4212(3)	$\frac{1}{2}$	1.000	0.0104(8)
Oc	2d	$\frac{1}{2}$	0	$\frac{1}{2}$	0.57(3)	0.019(2)
Oc*	4h	0.445(4)	0.060(4)	$\frac{1}{2}$	0.150(14)	0.008(5)

3. Results and discussion

The stability range of P-substituted samples (1A–1D) stretches up to 0.16 P atoms/unit cell at 1300°C. The stability range of Fe-substituted samples (2A–2C) stretches up to 0.30 Fe atoms/unit cell and confirms the previous results on iron[9] incorporation at 1300°C in a mullite structure. The coupled iron and phosphorus substitution according to $Al_{6-y/2}Fe_ySi_{2-y}P_{y/2}O_{13}$ stoichiometry evidences a minor incorporation degree of both Fe and P (respectively 0.15 and 0.075 atoms/unit cell) in respect to single substitutions.

Table 8
Structural results of the refinement on sample 3A ($Al_{5.9}Fe_{0.2}Si_{1.8}P_{0.1}O_{13}$)

	Wyckoff site	*x*/*a*	*y*/*b*	*z*/*c*	Fractional occupancy	U_{iso} (Å^3)
Al (1)	2a	0	0	0	0.982(3)	0.0071(5)
Fe (1)	2a	0	0	0	0.018(3)	0.0071(5)
Al-T	4h	0.1490(2)	0.3407(2)	$\frac{1}{2}$	0.505(2)	0.0082(4)
Fe-T	4h	0.1490(2)	0.3407(2)	$\frac{1}{2}$	0.025(1)	0.0082(4)
Si-T	4h	0.1490(2)	0.3407(2)	$\frac{1}{2}$	0.274(2)	0.0082(4)
P-T	4h	0.1490(2)	0.3407(2)	$\frac{1}{2}$	0.018(2)	0.0082(4)
Al-T*	4h	0.265(1)	0.2088(9)	$\frac{1}{2}$	0.110(2)	0.017(2)
Fe-T*	4h	0.265(1)	0.2088(9)	$\frac{1}{2}$	0.004(2)	0.017(2)
Si-T*	4h	0.265(1)	0.2088(9)	$\frac{1}{2}$	0.064(2)	0.017(2)
P-T*	4h	0.265(1)	0.2088(9)	$\frac{1}{2}$	0.001(2)	0.017(2)
Od	4g	0.1266(4)	0.2196(3)	0	1.000	0.0132(9)
Oab	4h	0.3572(4)	0.4230(3)	$\frac{1}{2}$	1.000	0.0093(7)
Oc	2d	$\frac{1}{2}$	0	$\frac{1}{2}$	0.58(3)	0.021(2)
Oc*	4h	0.446(4)	0.056(4)	$\frac{1}{2}$	0.15(2)	0.015(6)

Table 9
Atomic distances calculated from the structural model resulting from the refinement of the three samples. It is possible a comparison with the results obtained on the single crystal refinement of a 2:1 mullite in Ref. 5

	Interatomic distances			
Atoms	Sample 1D	Sample 2C	Sample 3A	Ref [5] (2:1 mullite)
Octahedral – Od	1.9482×2	1.9481×2	1.9435×2	1.9366(9)× 2
Octahedral – Oab	1.9057×4	1.9032×4	1.8990×4	1.8936(5)×4
T – Od	1.7240×2	1.7286×2	1.7278×2	1.7273(5)×2
T – Oab	1.6840	1.7031	1.6978	1.7102(8)
T – Oc	1.6733	1.6644	1.6667	1.6676(2)
T* – Od	1.7840×2	1.7974×2	1.7851×2	1.7727(7)×2
T* – Oab	1.7775	1.8059	1.7916	1.8166(11)
T* – Oc*	1.6400	1.7610	1.8106	1.8522(41)

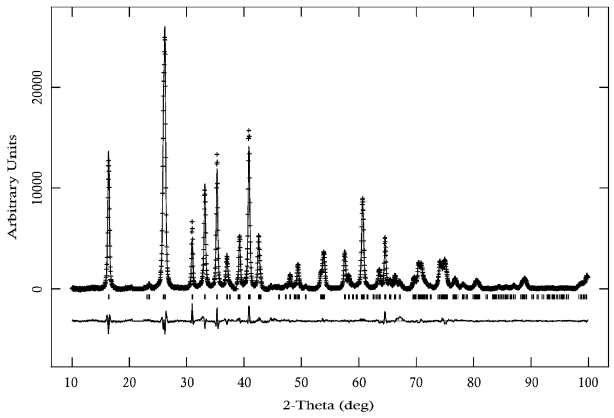

Fig. 3. Rietveld refinement profile relative to sample 1D.

Rietveld analysis allowed us to understand the structural details of synthesized mullite-like phases. First of all the refinement on site occupancies gave us direct evidence of the distribution of ions incorporated in the structure, which is then indirectly confirmed by the variation of bond distances. The partition of the different incorporated elements (Al, Fe, Si) onto the Al–T–T* sites by effect of the different substitutions is not straightforward. Table 10 summarizes the occupation for the three limit terms of the solid solutions.

As can be seen in Table 10, iron atoms preferably occupy tetrahedral T positions in the coupled substitution, while they tend to be equally distributed over Al and T sites in simple $Fe^{3+} \rightarrow Al^{3+}$ exchange. The decrease of tetrahedral/octahedral ratio between occupation with iron incorporation is evident in the work by Schneider and Rager.[9] Mössbauer spectroscopy gave a semi-quantitative support to infer the cation distribution on two environmentally-different sites (tetrahedral and octahedral) by means of the isomer shift (Table 4) of deconvoluted peaks.[16] Phosphorous is always incorporated almost completely on T site. A further indirect evidence of cation incorporation may be deduced from the increased b and c lattice parameters (Table 5), according to what was reported in Ref. 10

Simple considerations on fundamental substitution $2Al^{3+} + \square \rightarrow 2Si^{4+} + O_2$ allow the deduction of the relation between site occupancy and composition variable x (oxygen vacancies/unit cell, $x = 0.25$ for 3:2 mullites). The theoretical values of Oc and Oc* occupancies[5] are $Oc = 1–1.5x = 0.625$ and $Oc^* = 0.5x = 0.125$. The similarity between expected and calculated values of Oc and Oc* occupancies is an additional support to the goodness of structural analysis (Tables 6–8).

4. Conclusions

The intrinsic difficulty of the mullite structure resides in its lacunar and incommensurate character, that causes the average structure to contains, apparently, positionally disordered atoms.

The employed preparative route of the mullite-like phases permits the incorporation of ions in the structure at low temperature (1300°C), due to the nearly molecular level mixing of reactants. Furthermore the low preparation temperature avoids the P_2O_5 sublimation, maintaining the compositional stoichiometry during the heat treatment.

The substitutional range and the accurate diffraction data analysis produced evidences on the new, coupled P and Fe substituted in a mullite-like phase, while the results on the single substitution confirmed previous work about iron[9] incorporation.

References

1. Bowen, N. L. and Greig, J. W., The system Al_2O_3–SiO_2. *J. Am. Ceram. Soc.,* 1924, **7**(4), 238–254.
2. Sadanaga, R., Tokonami, M. and Takéuchi, Y., The structure of mullite, 2Al2O3·SiO2, and relationships with the structure of sillimanite and andalusite. *Acta Cryst.,* 1962, **15**, 65–68.
3. Burnham, C. W., The crystal structure of mullite. *Carnegie Institution of Washington Year Book,* 1964, **63**, 223–228.
4. Durovic, S., Refinement of the crystal structure of mullite. *Chemicke Zvesti,* 1969, **23**, 113–128.
5. Angel, R. J. and Prewitt, C. T., Crystal structure of mullite: a reexamination of the average structure. *Am. Min.,* 1986, **71**, 1476–1482.
6. Bowen, N. L., Greig, J.W. and Zies, E. G., Mullite, a silicate of Al_2O_3. *J. Wash. Acad. Sci., Ceram. Soc.,* 1924, **14** (9), 183–191; *Ceram. Abs*., 1924, **3** (11), 327.
7. Brownell, W. E., Subsolidus relations between mullite and iron oxide. *J. Am. Ceram. Soc.,* 1958, **41**(6), 226–230.

Table 10
Summary of incorporation of Fe and P in the various sites, calculated by means of Rietveld refinement

Ion	Site	Occupancy (at. %)		
		$\frac{1}{2}Al^{3+} + \frac{1}{2}P^{5+} \rightarrow Si^{4+}$	$Fe^{3+} \rightarrow Al^{3+}$	$\frac{1}{2}Al^{3+} + \frac{1}{2}P^{5+} \rightarrow Si^{4+}$ and $Fe^{3+} \rightarrow Al^{3+}$
Fe	Octahedral	–	47%	24%
	T	–	50%	66%
	T*	–	3%	10%
P	T	100%	–	95%
	T*	0%	–	5%

8. Murthy, M. K. and Hummel, F. A., X-ray study of the solid solution of TiO_2, Fe_2O_3 and Cr_2O_3 in mullite ($3Al_2O_3 \cdot 2SiO_2$). *J. Am. Ceram. Soc.,* 1960, **43**(5), 267–273.
9. Schneider, H. and Rager, H., Iron incorporation in mullite. *Ceram. Int.,* 1986, **12**(3), 117–125.
10. Chaudhuri, S. P. and Patra, S. K., Preparation and characterisation of transition metal ion doped mullite. *Br. Ceram. Trans.,* 1997, **96**(3), 105–111.
11. Mazza, D., Delmastro, A. and Ronchetti, S., Co, Ni, Cu aluminants supported on mullite precursors via a solid state reaction. *J. Eur. Ceram. Soc.,* 2000, **20**, 699–706.
12. Mazza, D., Ronchetti, S., Delmastro, A., Tribaudino, M. and Kockelmann, W., Silica-free mullite structures in the Al_2O_3–B_2O_3–P_2O_5 ternary system, *Chem. Mat.*, in press.
13. Shannon, R. D. and Prewitt, C. T., Effect of ionic radii in oxides and fluorides. *Acta Cryst.,* 1969, **B25**, 925–945.
14. Mazza, D., Lucco-Borlera, M., Busca, G. and Delmastro, A., High-quartz solid-solution phases from xerogels with composition $2MgO \cdot 2Al_2O_3 \cdot 5SiO_2$ (μ-cordierite) and $Li_2O \cdot Al_2O_3 \cdot nSiO_2$ ($n = 2$–4) (β-Eucryptite): characterization by XRD, FTIR and surface measurement. *J. Eur. Ceram. Soc.,* 2000, **11**, 299–308.
15. Larson, A. C. and Von Dreele, R. B., *General Structure Analysis System (GSAS)*. Los Alamos National Laboratory Report, 2000, LAUR 86-748.
16. Coey, J. M. D., Mössbauer spectroscopy of silicate minerals. In *Mössbauer Spectroscopy Applied to Inorganic Chemistry,* Vol. 1, ed. G.J Long. Plenum, New York and London, 1984, pp. 450 and 479.